William & Mary
CHARTERED 1693

W&M ScholarWorks

Arts & Sciences Articles

Arts and Sciences

2012

New Measurements of High-Momentum Nucleons and Short-Range Structures in Nuclei

N. Fomin

N. Fomin

M. M. Dalton

C. Perdrisat
William & Mary, perdrisa@jlab.org

Follow this and additional works at: https://scholarworks.wm.edu/aspubs

Recommended Citation

Fomin, N., Arrington, J., Asaturyan, R., Benmokhtar, F., Boeglin, W., Bosted, P., ... & Clasie, B. (2012). New measurements of high-momentum nucleons and short-range structures in nuclei. Physical review letters, 108(9), 092502.

This Article is brought to you for free and open access by the Arts and Sciences at W&M ScholarWorks. It has been accepted for inclusion in Arts & Sciences Articles by an authorized administrator of W&M ScholarWorks. For more information, please contact scholarworks@wm.edu.

New Measurements of High-Momentum Nucleons and Short-Range Structures in Nuclei

N. Fomin,[1,2,3] J. Arrington,[4] R. Asaturyan,[5,*] F. Benmokhtar,[6] W. Boeglin,[7] P. Bosted,[8] A. Bruell,[8] M. H. S. Bukhari,[9] M. E. Christy,[8] E. Chudakov,[8] B. Clasie,[10] S. H. Connell,[11] M. M. Dalton,[3] A. Daniel,[9] D. B. Day,[3] D. Dutta,[12,13] R. Ent,[8] L. El Fassi,[4] H. Fenker,[8] B. W. Filippone,[14] K. Garrow,[15] D. Gaskell,[8] C. Hill,[3] R. J. Holt,[4] T. Horn,[6,8,16] M. K. Jones,[8] J. Jourdan,[17] N. Kalantarians,[9] C. E. Keppel,[8,18] D. Kiselev,[17] M. Kotulla,[17] R. Lindgren,[3] A. F. Lung,[8] S. Malace,[18] P. Markowitz,[7] P. McKee,[3] D. G. Meekins,[8] H. Mkrtchyan,[5] T. Navasardyan,[5] G. Niculescu,[19] A. K. Opper,[20] C. Perdrisat,[21] D. H. Potterveld,[4] V. Punjabi,[22] X. Qian,[13] P. E. Reimer,[4] J. Roche,[20,8] V. M. Rodriguez,[9] O. Rondon,[3] E. Schulte,[4] J. Seely,[10] E. Segbefia,[18] K. Slifer,[3] G. R. Smith,[8] P. Solvignon,[8] V. Tadevosyan,[5] S. Tajima,[3] L. Tang,[8,18] G. Testa,[17] R. Trojer,[17] V. Tvaskis,[18] W. F. Vulcan,[8] C. Wasko,[3] F. R. Wesselmann,[22] S. A. Wood,[8] J. Wright,[3] and X. Zheng[3,4]

[1]*Los Alamos National Laboratory, Los Alamos, New Mexico 87545, USA*
[2]*University of Tennessee, Knoxville, Tennessee 37996, USA*
[3]*University of Virginia, Charlottesville, Virginia 22904, USA*
[4]*Physics Division, Argonne National Laboratory, Argonne, Illinois 60439, USA*
[5]*Alikhanyan National Scientific Laboratory, Yerevan 0036, Armenia*
[6]*University of Maryland, College Park, Maryland 20742, USA*
[7]*Florida International University, Miami, Florida 33199, USA*
[8]*Thomas Jefferson National Laboratory, Newport News, Virginia 23606, USA*
[9]*University of Houston, Houston, Texas 77204, USA*
[10]*Massachusetts Institute of Technology, Cambridge, Massachusetts 02139, USA*
[11]*University of Johannesburg, Johannesburg, 2008, South Africa*
[12]*Mississippi State University, Mississippi State, Mississippi 39759, USA*
[13]*Duke University, Durham, North Carolina 27708, USA*
[14]*Kellogg Radiation Laboratory, California Institute of Technology, Pasadena, California 91106, USA*
[15]*TRIUMF, Vancouver, BC V6T 2A3, Canada*
[16]*Catholic University of America, Washington, D.C. 20064, USA*
[17]*Basel University, 4056 Basel, Switzerland*
[18]*Hampton University, Hampton, Virginia 23668, USA*
[19]*James Madison University, Harrisonburg, Virginia 22801, USA*
[20]*Ohio University, Athens, Ohio 22801, USA*
[21]*College of William and Mary, Williamsburg, Virginia 23185, USA*
[22]*Norfolk State University, Norfolk, Virginia 23504, USA*

(Received 18 July 2011; published 29 February 2012)

We present new measurements of electron scattering from high-momentum nucleons in nuclei. These data allow an improved determination of the strength of two-nucleon correlations for several nuclei, including light nuclei where clustering effects can, for the first time, be examined. The data also include the kinematic region where three-nucleon correlations are expected to dominate.

DOI: 10.1103/PhysRevLett.108.092502 PACS numbers: 25.30.Fj

A complete understanding of the complex structure of nuclei is one of the major goals of nuclear physics. Significant progress has been made over the past decade, yielding *ab initio* techniques for calculating the structure of light nuclei based on the nucleon-nucleon (and three-nucleon) interactions [1,2], along with methods that extend to heavier nuclei. One of the least understood aspects of nuclei is their short-range structure, where nucleons are close together and interact via the poorly constrained repulsive core of the N-N interaction, yielding high-momentum nucleons. Measurements of scattering from these high-momentum nucleons provides direct access to the short-range structure of nuclei [3–5].

This regime can be accessed through inclusive quasielastic (QE) scattering in which a virtual photon of energy ν and momentum $\vec{q}$ is absorbed on a nucleon. Elastic scattering from a nucleon at rest is kinematically well defined and corresponds to $x \equiv Q^2/2M_N\nu = 1$, where M_N is the nucleon mass and $Q^2 = q^2 - \nu^2$. For QE scattering from a nucleon moving in the nucleus, the cross section is peaked around $x = 1$ and has a width characterized by the Fermi momentum (k_F) with tails that extend to higher momenta. Inclusive scattering at high Q^2 minimizes final-state interactions while low energy transfer suppresses inelastic contributions. Thus, inclusive scattering at large Q^2 and low ν, corresponding to $x > 1$, provides relatively clean isolation of

 © 2012 American Physical Society

scattering from high-momentum nucleons. We present new measurements in this kinematic region for a range of light and heavy nuclei which expose the high-momentum, short-distance structure in nuclei.

Experiment E02-019 was performed in Hall C at Jefferson Lab (JLab). A continuous wave electron beam of 5.766 GeV at currents of up to 80 μA impinged on targets of ^{2}H, ^{3}He, ^{4}He, Be, C, Cu, and Au. Scattered electrons were detected using the High Momentum Spectrometer (HMS) for electron scattering angles $\theta_e =$ 18°, 22°, 26°, 32°, 40°, and 50°. A detailed description of the measurement and the analysis is available in Refs. [6,7].

Most of the significant uncertainties are discussed in Ref. [6], but for the very large x data used in this analysis, some corrections become more significant. For the cryogenic targets, contributions from scattering in the aluminum endcaps of the target can be large, up to ~50% for the ^{3}He target. This is subtracted using measurements from an aluminum "dummy" target, after corrections are made for the difference in radiation lengths between the real and dummy targets. A systematic uncertainty equal to 3% of the subtraction is included to account for uncertainties in the knowledge of the relative thickness of the targets. The cross sections were also corrected for Coulomb effects (up to 10% for gold) using the effective momentum approximation (EMA) calculation of Ref. [8]. We apply a conservative 20% systematic uncertainty to this correction to account for uncertainty in the EMA. The uncertainty due to possible offsets in the beam energy or spectrometer kinematics is $\lesssim 5\%$ in the cross sections for $x < 2$, but $\lesssim 2\%$ in the target ratios.

Inclusive cross sections at $x > 1$ are often analyzed using y-scaling [4,5,9,10]. For high-Q^2 quasielastic scattering with no final-state interactions (FSIs), the inclusive cross section reduces to a product of the electron-nucleon elastic cross sections, σ_{eN}, and a scaling function, $F(y, Q^2)$. We determine y from energy conservation:

$$\nu + M_A - \epsilon_s = [M_N^2 + (q + y)^2]^{1/2} + (M_{A-1}^2 + y^2)^{1/2}, \quad (1)$$

where M_A and M_{A-1} are the masses of the target and spectator $(A - 1)$ nuclei and ϵ_s is the minimum separation energy. This corresponds to the minimum initial momentum of the struck nucleon. The scaling function $F(y, Q^2)$ is extracted from the cross section,

$$F(y, Q^2) = \frac{d^2\sigma}{d\Omega d\nu}[Z\sigma_p + N\sigma_n]^{-1}\frac{q}{[M_N^2 + (y + q)^2]^{1/2}}, \quad (2)$$

and it has be shown that $F(y, Q^2)$ depends only on y at large Q^2 values for a wide range of nuclei and momenta [10,11]. Further, if the assumption of scattering with an unexcited $(A - 1)$ spectator is correct, then $F(y)$ is related to the nucleon momentum distribution, $n(k)$: $\frac{dF(k)}{dk} \approx -2\pi k n(k)$.

Figure 1 shows the momentum distribution determined from the new E02-019 data on the deuteron where we have taken σ_p and σ_n to be the off-shell (cc1) cross sections as developed in Ref. [12] using parameterizations of the neutron [13] and proton [14] form factors. Because the inelastic contribution can become significant for small k and large Q^2, we exclude the two largest Q^2 settings and limit the remaining data to regions where the estimated inelastic contribution $\lesssim 5\%$. We find that the extracted momentum distribution is Q^2 independent, although our direct limits on the Q^2 dependence are roughly 20–30% for $k \leq 300$ MeV/c, increasing to ~40% at 400 MeV/c and ~80% at 600 MeV/c. The limits on the Q^2 dependence at our higher Q^2 values, as well as the agreement with calculations up to $k \approx 600$ MeV/c, support the idea that the FSI contributions are much smaller than at low Q^2 values, where they can increase the PWIA cross section by a factor of 2–3 or more [11,15–17]. The excess in the extracted momentum distribution at $k \approx 0.3$ GeV/c is present in several previous extractions from both inclusive and $D(e, e'p)$ measurements [4,18].

While the y-scaling criteria appear to be satisfied for the deuteron, the assumption of an unexcited spectator in Eq. (1) breaks down for heavier nuclei. In the deuteron, the spectator is a single nucleon while for heavier nuclei, the final state can involve breakup or excitations of the spectator $(A - 1)$ system, especially in the case of scattering from a preexisting SRC which should yield a high-momentum spectator in the final state. There have been many attempts to correct for this effect via a modification of the scaling variable [5,19–24] or by calculation of an explicit correction to the scaling function using a spectral function to account for the excitation of the residual system [24,25] which provide improved but model-dependent

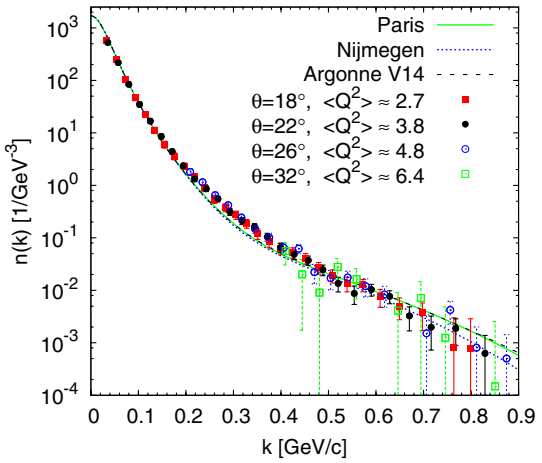

FIG. 1 (color online). Extracted deuteron momentum distribution (points) and calculations (curves) using three different N-N potentials [39–41]. Note that the Paris and Av14 calculations are nearly indistinguishable on this scale.

extractions of $n(k)$. We can avoid this model dependence by making comparisons between nuclei in a region where the kinematics limit the scattering to $k > k_F$ [5,26]. If these high-momentum components are related to two-nucleon short-range correlations (2N-SRCs), where two nucleons have a large relative momentum but a small total momentum due to their hard two-body interaction, then they should yield the same high-momentum tail whether in a heavy nucleus or a deuteron.

The first detailed study of SRCs combined data interpolated to fixed kinematics from different experiments at SLAC [26]. A plateau was seen in the ratio $(\sigma_A/A)/(\sigma_D/2)$ that was roughly A independent for A $\geq$ 12, but smaller for ^{3}He and ^{4}He. Measurements from Hall B at JLab showed similar plateaus [27,28] in $A/^3$He ratios for $Q^2 \geq 1.4$ GeV^2. A previous JLab Hall C experiment at 4 GeV [11,29] measured scattering from nuclei and deuterium at larger Q^2 values than SLAC or CLAS, but had limited statistics for deuterium. While these measurements provided significant evidence for the presence of SRCs, precise A/D ratios for several nuclei, covering the desired range in x and Q^2, are limited.

Figure 2 shows the cross section ratios from E02-019 for the $\theta_e = 18°$ data. For $x > 1.5$, the data show the expected plateau, although the point at $x = 1.95$ is always high because one is approaching the kinematic threshold for scattering from the deuteron at $x = M_D/M_p \approx 2$. This rise was not observed in previous measurements; the SLAC data did not have sufficient statistics to see the rise, while the CLAS measurements took ratios of heavy nuclei to ^{3}He, where the cross section does not go to zero for $x \rightarrow 2$. Table I gives the ratio in the plateau region for a range of nuclei at all Q^2 values where there were sufficient large-x data. We apply a cut in x to isolate the plateau region, although the onset of scaling in x varies somewhat with Q^2. The start of the plateau is independent of Q^2 when taken as a function of α_{2n},

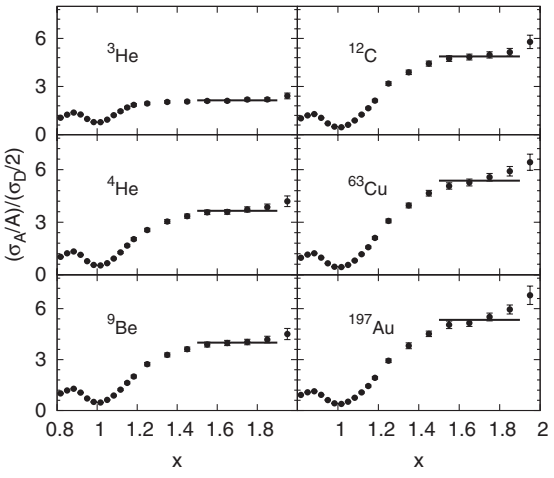

FIG. 2. Pernucleon cross section ratios vs x at $\theta_e = 18°$.

TABLE I. $r(A, D) = (2/A)\sigma_A/\sigma_D$ in the $2N$ correlation region ($x_{\min} < x < 1.9$). We take a conservative value of $x_{\min} = 1.5$ at 18°, corresponding to $\alpha_{2n} = 1.275$, and use this to set $x_{\min}$ at 22° and 26°. The last column is the ratio at 18° after subtracting the inelastic contribution as estimated by a simple convolution model (and applying a 100% systematic uncertainty on the correction).

A	$\theta_e = 18°$	$\theta_e = 22°$	$\theta_e = 26°$	Inel. sub.
^{3}He	2.14 ± 0.04	2.28 ± 0.06	2.33 ± 0.10	2.13 ± 0.04
^{4}He	3.66 ± 0.07	3.94 ± 0.09	3.89 ± 0.13	3.60 ± 0.10
Be	4.00 ± 0.08	4.21 ± 0.09	4.28 ± 0.14	3.91 ± 0.12
C	4.88 ± 0.10	5.28 ± 0.12	5.14 ± 0.17	4.75 ± 0.16
Cu	5.37 ± 0.11	5.79 ± 0.13	5.71 ± 0.19	5.21 ± 0.20
Au	5.34 ± 0.11	5.70 ± 0.14	5.76 ± 0.20	5.16 ± 0.22
$\langle Q^2 \rangle$	2.7 GeV^2	3.8 GeV^2	4.8 GeV^2	
$x_{\min}$	1.5	1.45	1.4	

$$\alpha_{2n} = 2 - \frac{\nu - q + 2M_N}{2M_N}\left(1 + \sqrt{1 - M_N^2/W_{2n}^2}\right), \quad (3)$$

($W_{2n}^2 = 4M_N^2 + 4M_N\nu - Q^2$) which corresponds to the light-cone momentum fraction of the struck nucleon assuming that the photon is absorbed by a single nucleon from a pair of nucleons with zero net momentum [26]. We take the ratio for $x_{\min} < x < 1.9$, such that $x_{\min}$ corresponds to a fixed value of α_{2n}.

There are small inelastic contributions at the higher Q^2 values, even for $x > 1.5$. A simple convolution model [7] predicts an inelastic contribution of 1%–3% at 18° and 5%–10% at 26°. This may explain the small systematic Q^2 dependence in the extracted ratios seen in Table I. Further results on the role of SRCs will be based on the 18° data, with the inelastic contributions subtracted (including a 100% model dependence uncertainty), to minimize the size and uncertainty of the inelastic correction.

Calculations of inclusive FSIs generally show them to decrease rapidly with increasing Q^2. However, the effects can still be important at high Q^2 for $x > 1$. While at least one calculation suggests that the FSI is A dependent [30], most indicate that the FSI contributions which do not decrease rapidly with Q^2 are limited to FSI between the nucleons in the initial-state SRC [3,5,26,31–33]. In this case, the FSI corrections are identical for 2N-SRCs in the deuteron or heavy nuclei, and cancel when taking the ratios. Our y-scaling analysis of the deuteron cross sections (Fig. 1) suggests that the FSIs are relatively small for the deuteron, and the ratios shown in Table I have only a small Q^2 dependence, consistent with the estimated inelastic contributions, supporting the standard assumption that any FSIs in the plateau region largely cancel in taking the target ratios.

In the absence of large FSI effects, the cross section ratio σ_A/σ_D yields the strength of the high-momentum tail of the momentum distribution in nucleus A relative to a deuteron. If the high-momentum contribution comes

entirely from quasielastic scattering from a nucleon in an n-p SRC at rest, then this ratio represents the contribution of $2N$-SRCs to the nuclear wave function, relative to the deuteron, $R_{2N}(A, D)$. However, the distribution of the high-momentum nucleons in the SRC will be modified by the motion of the pair in the nucleus. We use the convolution calculation and realistic parameterizations for the c.m. motion and for SRC distributions from Ref. [33] to calculate this smearing and find that it generates an enhancement of the high-momentum tail of approximately 20% for Iron and roughly scales with the size of the total pair momentum. To obtain $R_{2N}(A, D)$, we use the inelastic-subtracted cross section ratios and remove the smearing effect of the center-of-mass (c.m.) motion of the 2N-SRC pairs. The 20% correction for iron is scaled to the other nuclei based on the A dependence of the pair motion. To first order, the c.m. motion "smears out" the high-momentum tail (which falls off roughly exponentially), producing an overall enhancement of the ratio in the plateau region. In a complete calculation, the correction can also have some small x dependence in this region which can potentially distort the shape of the ratio. However, both the data and recent calculations [19,34,35] suggest that any x dependence of the ratio in this region is relatively small. When removing the effect of the c.m. motion, we apply an uncertainty equal to 30% of the calculated correction (50% for ^{3}He) to account for the overall uncertainty in calculating the smearing effect, the uncertainty in our assumed A dependence of the effect, and the impact of the neglected x dependence on the extracted ratio.

After correcting the measured ratios for the enhancement due to motion of the pair, we obtain R_{2N}, given in Table II, which represents the relative likelihood of a nucleon in nucleus A to be in a high relative momentum pair compared to a nucleon in the deuteron. It also provides updated results from previous experiments after applying c.m. motion corrections and removing the ~15% "isoscalar" correction applied in the previous works. This correction was based on the assumption that the high-momentum tails would have greater neutron contributions for $N > Z$ nuclei, but the dominance of isosinglet pairs [2,36] implies that the tail will have equal proton and neutron contributions. The CLAS ratios are somewhat low compared to the other extractions, which could be a result of the lower $\alpha_{\min}$ values. If α_{2n} is not high enough to fully isolate $2N$-SRCs, one expects the extracted ratio will be somewhat smaller. Note that the previous data do not include corrections or uncertainties associated with inelastic contributions or Coulomb distortion, which is estimated to be up to 6% for the CLAS iron data and similar for the lower Q^2 SLAC data.

TABLE II. Extracted values of $R_{2N}(A)$ from this work and the SLAC [26] and CLAS [28] data, along with the c.m. motion correction factor $F_{\rm CM}$ we apply: $R_{2N}(A) = r(A, D)/F_{\rm CM}$. The SLAC and CLAS results have been updated to be consistent with the new extraction except for the lack of Coulomb correction and inelastic subtraction (see text for details).

A	R_{2N} (E02-019)	SLAC	CLAS	$F_{\rm CM}$
^{3}He	1.93 ± 0.10	1.8 ± 0.3	···	1.10 ± 0.05
^{4}He	3.02 ± 0.17	2.8 ± 0.4	2.80 ± 0.28	1.19 ± 0.06
Be	3.37 ± 0.17	···	···	1.16 ± 0.05
C	4.00 ± 0.24	4.2 ± 0.5	3.50 ± 0.35	1.19 ± 0.06
Cu(Fe)	4.33 ± 0.28	(4.3 ± 0.8)	(3.90 ± 0.37)	1.20 ± 0.06
Au	4.26 ± 0.29	4.0 ± 0.6	···	1.21 ± 0.06
$\langle Q^2 \rangle$	~2.7 GeV^2	~1.2 GeV^2	~2 GeV^2	
$x_{\min}$	1.5	···	1.5	
$\alpha_{\min}$	1.275	1.25	1.22–1.26	

Previous extractions of the strength of $2N$-SRCs found a slow increase of R_{2N} with A in light nuclei, with little apparent A dependence for $A \geq 12$. The additional corrections applied in our extraction of $2N$-SRC contributions do not modify these basic conclusions, but these corrections, along with the improved precision in our extraction, furnishes a more detailed picture of the A dependence. In a mean-field model, one would expect the frequency for two nucleons to be close enough together to form an $2N$-SRC to be proportional to the average density of the nucleus [3]. However, while the density of ^{9}Be is similar to ^{3}He, yet its value of R_{2N} is much closer to that of the denser nuclei ^{4}He and ^{12}C, demonstrating that the SRC contributions do not simply scale with density. This is very much like the recently observed A dependence of the EMC effect [37], where ^{9}Be was found to behave like a denser nucleus due to its significant cluster structure. It seems natural that cluster structure would be important in the short-range structure and contribution of SRCs in nuclei, but this is the first such experimental observation.

For $A/^3$He ratios above $x = 2$, one expects the $2N$-SRC contributions to become small enough that $3N$-SRCs may eventually dominate. $2N$-SRCs are isolated by choosing x and Q^2 such that the minimum initial momentum of the struck nucleon is larger than k_F [26], but it is not clear what kinematics are required to sufficiently suppress $2N$-SRC contributions [5], and larger Q^2 values may be required to isolate $3N$-SRCs. Figure 3 shows the ^{4}He/^{3}He ratio at $\theta_e = 18°$, along with the CLAS ratios [28] (leaving out their isoscalar correction). The ratios in the $2N$-SRC region are in good agreement. Even with the large uncertainties, it is clear that our ratio at $x > 2.25$ is significantly higher than in the CLAS measurement. On the other hand, a similar analysis using preliminary results from SLAC (Fig. 8.3 from Ref. [31]) found a ^{4}He/^{3}He cross section ratio that is independent of Q^2 between 1.0 and 2.4 GeV^2 and falls in between our result and the CLAS data. A recently completed experiment [38] will map out the x and Q^2 dependence in the $3N$-SRC region with high precision.

In summary, we have presented new, high-Q^2 measurements of inclusive scattering from nuclei at $x > 1$. We

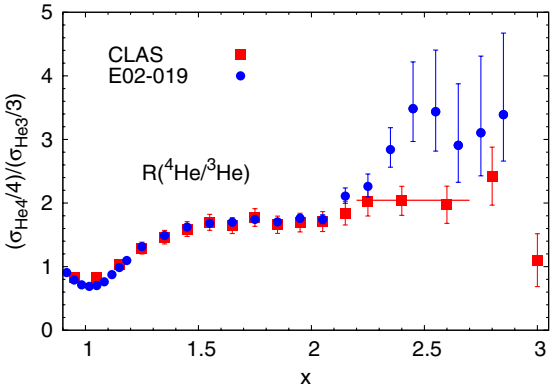

FIG. 3 (color online). The ^{4}He/^{3}He ratios from E02-019 ($Q^2 \approx 2.9$ GeV^2) and CLAS ($\langle Q^2 \rangle \approx 1.6$ GeV^2); errors are combined statistical and systematic uncertainties. For $x > 2.2$, the uncertainties in the ^{3}He cross section are large enough that a one-sigma variation of these results yields an asymmetric error band in the ratio. The error bars shown for this region represent the central 68% confidence level region.

examined the high-momentum tail of the deuteron momentum distribution and used target ratios at $x > 1$ to examine the A and Q^2 dependence of the contribution of $2N$-SRCs. The SRC contributions are extracted with improved statistical and systematic uncertainties and with new corrections that account for isoscalar dominance and the motion of the pair in the nucleus. The ^{9}Be data show a significant deviation from predictions that the $2N$-SRC contribution should scale with density, presumably due to strong clustering effects. At $x > 2$, where $3N$-SRCs are expected to dominate, our $A/^3$He ratios are significantly higher than the CLAS data and suggest that contributions from $3N$-SRCs in heavy nuclei are larger than previously believed.

We thank the JLab technical staff and accelerator division for their contributions. This work supported by the NSF and DOE, including contract DE-AC02-06CH11357 and contract DE-AC05-06OR23177 under which JSA, LLC operates JLab, and the South African NRF.

*Deceased.

[1] J. Vary, Proc. Sci. LC2010 (2010), 001.
[2] R. Schiavilla, R. B. Wiringa, S. C. Pieper, and J. Carlson, Phys. Rev. Lett. **98**, 132501 (2007).
[3] L. L. Frankfurt and M. I. Strikman, Phys. Rep. **76**, 215 (1981).
[4] D. B. Day, J. S. McCarthy, T. W. Donnelly, and I. Sick, Annu. Rev. Nucl. Part. Sci. **40**, 357 (1990).
[5] J. Arrington, D. Higinbotham, G. Rosner, and M. Sargsian, arXiv:1104.1196.
[6] N. Fomin *et al.*, Phys. Rev. Lett. **105**, 212502 (2010).
[7] N. Fomin, Ph.D. thesis, University of Virginia, 2007, arXiv:0812.2144.
[8] A. Aste, C. von Arx, and D. Trautmann, Eur. Phys. J. A **26**, 167 (2005).
[9] E. Pace and G. Salmè, Phys. Lett. B **110**, 411 (1982).
[10] D. B. Day *et al.*, Phys. Rev. Lett. **59**, 427 (1987).
[11] J. Arrington *et al.*, Phys. Rev. Lett. **82**, 2056 (1999).
[12] T. DeForest, Nucl. Phys. **A392**, 232 (1983).
[13] J. J. Kelly, Phys. Rev. C **70**, 068202 (2004).
[14] J. Arrington, W. Melnitchouk, and J. A. Tjon, Phys. Rev. C **76**, 035205 (2007).
[15] R. Arnold *et al.*, Phys. Rev. Lett. **61**, 806 (1988).
[16] C. Ciofi degli Atti, L. P. Kaptari, and D. Treleani, Phys. Rev. C **63**, 044601 (2001).
[17] K. Kim and L. Wright, Phys. Rev. C **76**, 044613 (2007).
[18] A. Bussiere *et al.*, Nucl. Phys. A **365**, 349 (1981).
[19] C. Ciofi degli Atti and C. B. Mezzetti, Phys. Rev. C **79**, 051302 (2009).
[20] X.-D. Ji and J. Engel, Phys. Rev. C **40**, R497 (1989).
[21] C. Ciofi degli Atti and G. B. West, arXiv:nucl-th/9702009.
[22] J. Arrington, arXiv:nucl-ex/0306016.
[23] J. Arrington, arXiv:nucl-ex/0602007.
[24] C. Ciofi degli Atti and G. B. West, Phys. Lett. B **458**, 447 (1999).
[25] C. Ciofi degli Atti, E. Pace, and G. Salme, Phys. Rev. C **43**, 1155 (1991).
[26] L. L. Frankfurt, M. I. Strikman, D. B. Day, and M. Sargsian, Phys. Rev. C **48**, 2451 (1993).
[27] K. S. Egiyan *et al.*, Phys. Rev. C **68**, 014313 (2003).
[28] K. S. Egiyan *et al.*, Phys. Rev. Lett. **96**, 082501 (2006).
[29] J. Arrington *et al.*, Phys. Rev. C **64**, 014602 (2001).
[30] O. Benhar *et al.*, Phys. Lett. B **343**, 47 (1995).
[31] L. L. Frankfurt and M. I. Strikman, Phys. Rep. **160**, 235 (1988).
[32] C. C. degli Atti and S. Simula, Phys. Lett. B **325**, 276 (1994).
[33] C. C. degli Atti and S. Simula, Phys. Rev. C **53**, 1689 (1996).
[34] C. B. Mezzetti, arXiv:1003.3650.
[35] C. B. Mezzetti, arXiv:1112.3185.
[36] R. Subedi *et al.*, Science **320**, 1476 (2008).
[37] J. Seely *et al.*, Phys. Rev. Lett. **103**, 202301 (2009).
[38] J. Arrington *et al.*, Jefferson Lab Experiment E08-014 (2008), http://www.jlab.org/exp_prog/proposals/08/PR-08-014.pdf.
[39] V. Stoks, R. Klomp, C. Terheggen, and J. de Swart, Phys. Rev. C **49**, 2950 (1994).
[40] M. Lacombe *et al.*, Phys. Lett. B **101**, 139 (1981).
[41] R. B. Wiringa, V. G. J. Stoks, and R. Schiavilla, Phys. Rev. C **51**, 38 (1995).